

## X-ray scattering evidence for the structural nature of fatigue in epitaxial $\text{Pb}(\text{Zr}, \text{Ti})\text{O}_3$ films

Carol Thompson<sup>a)</sup>

*Department of Physics, Northern Illinois University, DeKalb, Illinois 60115 and Materials Science Division, Argonne National Laboratory, Argonne, Illinois 60439*

A. Munkholm<sup>b)</sup>

*Chemistry Division, Argonne National Laboratory, Argonne, Illinois 60439*

S. K. Streiffer, G. B. Stephenson, K. Ghosh,<sup>c)</sup> J. A. Eastman, O. Auciello, and G.-R. Bai

*Materials Science Division, Argonne National Laboratory, Argonne, Illinois 60439*

M. K. Lee and C. B. Eom

*Department of Materials Science and Engineering, University of Wisconsin—Madison, Madison, Wisconsin 53706*

(Received 15 December 2000; accepted for publication 2 April 2001)

We have probed the microscopic distribution of  $180^\circ$  domains as a function of switching history in 40 nm epitaxial films of  $\text{Pb}(\text{Zr}_{0.30}\text{Ti}_{0.70})\text{O}_3$  by analyzing interference effects in the x-ray scattering profiles. These as-grown films exhibit voltage offsets (imprint) in the polarization hysteresis loops, coupled with a strongly preferred polarization direction in the virgin state. Our x-ray results are consistent with models attributing the loss of switchable polarization to the inhibition of the formation of oppositely polarized domains in a unipolar matrix. Using such model epitaxial films, we demonstrate that different microscopic ensembles of domains resulting from, for example, fatigue, may be resolved by this technique. © 2001 American Institute of Physics.

[DOI: 10.1063/1.1375001]

One of the limitations of utilizing ferroelectric films for applications such as nonvolatile memories, is the tendency of some materials, e.g.,  $\text{Pb}(\text{ZrTi})\text{O}_3$ , to exhibit a loss of switchable polarization with increasing switching cycles, a phenomenon known as fatigue. Fatigue may arise from several different underlying physical mechanisms. Two mechanisms are most frequently discussed.<sup>1</sup> In the first, fatigue occurs by pinning of ferroelectric domain walls within the bulk of a film containing a mixture of oppositely polarized domains. In the second, fatigue is the result of inhibition of the growth of oppositely polarized domains due to nucleus suppression at the film-electrode interfaces of a uniformly polarized matrix. By analysis of the electric field dependence of permittivity as a function of degree of fatigue in polycrystalline film, Colla *et al.*<sup>1</sup> have concluded that the primary fatigue mechanism under normal cycling conditions is nucleus suppression. Piezoresponse atomic force microscopy (AFM) studies<sup>2</sup> have found that the fatigued state can have a preferential polarization, and it has been found that fatigue can be reduced by asymmetric switching voltages.<sup>3</sup> These results also support a nucleus suppression model.

In this letter, we report x-ray interference characterizations of the domain configurations after successive polarization reversals in ferroelectric heterostructures incorporating top and bottom electrodes. Interference effects occurring in x-ray scattering profiles of high-quality epitaxial ferroelectric films are extremely sensitive to the distribution of oppositely

polarized ( $180^\circ$ ) domains. This method has been used previously to determine the unipolar character of the native  $180^\circ$  domain distribution for an epitaxial  $\text{PbTiO}_3$  film on  $\text{SrTiO}_3$ .<sup>4</sup> Here, we use this method to study the structural nature of fatigue in ferroelectric films. This x-ray technique provides direct characterization of the relative population of the two domains averaged over a macroscopic region, complementary to both electrical and AFM characterizations.

The interference effects upon which this scattering technique relies require very high structural coherency between the film and substrate, which serves as a phase reference. Therefore, we have investigated a model epitaxial heterostructure consisted of a 40 nm (001)  $\text{Pb}(\text{Zr}_{0.3}\text{Ti}_{0.7})\text{O}_3$  (PZT) film grown by metalorganic chemical vapor deposition,<sup>5</sup> on a 136 nm (001)  $\text{SrRuO}_3$  (SRO) film sputter deposited<sup>6</sup> on a (001)  $\text{SrTiO}_3$  (STO) substrate. The film had excellent crystalline quality, with a mosaic spread of  $0.009^\circ$  for the PZT 001 peak. The STO and SRO 001 mosaics were  $0.002^\circ$  and  $0.009^\circ$  respectively. (Pseudocubic axis notation is used for the SRO.)<sup>6</sup> The ferroelectric PZT film thickness was less than the critical thickness for strain relaxation by *a*-domain ( $90^\circ$ ) twins.<sup>7,8</sup> Planar 250  $\mu\text{m}$  diameter capacitor structures were formed by room temperature electron-beam evaporation of discrete polycrystalline silver top electrodes through a shadow mask onto the continuous oxide film.

High resolution x-ray scattering experiments were performed on the Basic Energy Sciences Synchrotron Radiation Center (BESSRC-CAT) undulator beamline 12ID-D at the Advanced Photon Source using monochromatic 14.5 keV x-rays ( $\lambda = 0.855 \text{ \AA}$ ). The incident x-ray beam, 30  $\mu\text{m}$  by 200  $\mu\text{m}$ , was aligned onto the center of a 250  $\mu\text{m}$  diameter ca-

<sup>a)</sup>Electronic mail: cthompson@niu.edu

<sup>b)</sup>Present address: Lumileds Lighting, San Jose, CA 95131.

<sup>c)</sup>Present address: Southwest Missouri State University, Springfield, MO 65804.

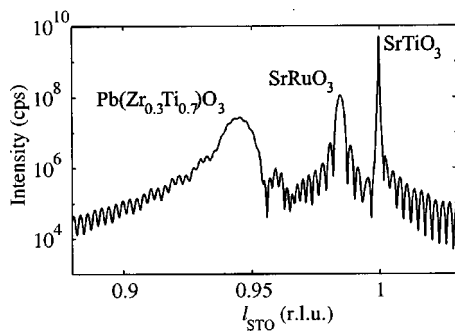


FIG. 1. X-ray scattering profile through the crystal truncation rod connecting the 001 peaks of the  $\text{Pb}(\text{Zr}_{0.3}\text{Ti}_{0.7})\text{O}_3$ ,  $\text{SrRuO}_3$ , and  $\text{SrTiO}_3$ . The reciprocal lattice units are relative to the  $\text{SrTiO}_3$  lattice,  $l_{\text{STO}} = q/q_{001}$ .

capacitor. At typical scattering angles near  $8.5^\circ$ , the illuminated area fit within the electrode area, minimizing the sampling of edge effects in the capacitor. No changes were seen in the leakage current levels or the reproducibility of the hysteresis loops during tests of extended exposure to the  $\approx 10^{10}$  cps x-ray flux, indicating that the electrical properties of the PZT films were not affected by the irradiation.

Because the surfaces and interfaces are smooth and have well-defined terminations with respect to the lattice, the x-ray scattering is extended in reciprocal space along a direction parallel to the surface normal. This extended scattering is termed a crystal truncation rod (CTR).<sup>9</sup> Figure 1 shows the x-ray scattering profile along the CTR through the 001 peaks of the PZT, SRO, and STO. The polycrystalline silver top electrode does not contribute to these CTR profiles because it is not sufficiently epitaxial with the oxide heterostructure. Two periods are seen in the oscillations of the CTR intensity. The shorter period is related to the thickness of the SRO layer, and the longer period to that of the thinner PZT layer. Note the asymmetries in the oscillations around the PZT and STO Bragg peak positions, and the beating due to interference between the oscillations from the SRO and PZT films. In principle, the profile of this complex scattering pattern may be analyzed to determine the configuration of parallel and antiparallel ( $180^\circ$ ) domains. Different domain distributions, including each limiting case of a single parallel or antiparallel domain, would generate a distinct CTR profile.<sup>4</sup> In this study, we simply used the x-ray interference scattering profiles as fingerprints of the domain configurations during the switching process.

We characterized the switching behavior of the films using the virtual ground measurement technique. A function generator supplied a triangle-wave driving voltage to the top electrode, and the current response of the sample was obtained through the bottom electrode. Figure 2(a) shows the 1 kHz  $I$ - $V$  hysteresis loop of the capacitor before it was poled for the first scattering experiment. We choose to present the data in this format because it yields a better visualization of the switching process as it occurs. Time integration of the current response can be used to generate the more standard hysteresis loop. The area under the peaks is proportional to the total switched polarization; the position of the peak maximum corresponds to the coercive field.<sup>10</sup> With this method, leakage currents were distinguishable from switching currents and frequencies from 0.1 Hz to 100 kHz could be used.

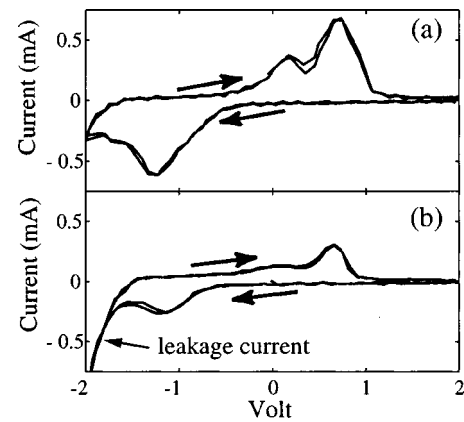


FIG. 2. Current-voltage characteristics at 1 kHz of the epitaxial 40 nm  $\text{Pb}(\text{Zr}_{0.3}\text{Ti}_{0.7})\text{O}_3$ : (a) prior to fatigue and (b) after fatigue.

We observe that the positions of the positive and negative current peaks are asymmetric with respect to zero applied field. This voltage shift is defined as imprint. Evidence in the literature suggests that epitaxial films of perovskite ferroelectrics can have unipolar character (strongly preferred polarization direction) in their as-grown state, and that the direction of the unipolarity correlates with the sense of the imprint.<sup>4,11,12</sup> Using AFM piezoresponse imaging, we have found that our films in their as-grown state were not composed of an equal distribution of parallel and antiparallel domains; but were unipolar.<sup>13</sup> The polarity of many of our films have been measured to be antiparallel to the surface normal, but films with parallel polarity have also been observed. The direction of polarity in the virgin structure as determined by AFM has always correlated with the sign of the voltage shift as observed in the electronic properties. Similar effects have been seen for sputtered films; however, the origin of the initial self-poling in that case is thought to be due to electrical fields applied during the deposition process and is not applicable to our samples.<sup>14</sup> The origin of this as-grown unipolarity in epitaxial films is unknown.

We defined an "easy" and a "difficult" state based on the asymmetry in the switching characteristics of the  $I$ - $V$  curves of Fig. 2. The film was easy to switch by applying positive voltage, but needed a larger magnitude of negative applied voltage to reverse the macroscopic polarization. Since the voltage axis corresponds to voltage applied to the top electrode with the bottom electrode kept at ground, the easy (positive applied voltage) state is associated with a polarization of the film antiparallel to the surface normal, while the difficult state corresponds to parallel polarization.

To characterize the domain distributions of the easy and difficult states, we measured the x-ray interference profiles of each state. In order to establish a well defined difficult domain state, films were poled using multiple repetitions of 1 kHz single-polarity  $-2$  V voltage pulses. Only a single  $+2$  V pulse was required to establish the easy state. After poling, the x-ray scattering pattern along the CTR was measured at zero applied voltage. The capacitor's switching characteristics were measured after each full x-ray profile was obtained. These measurements confirmed that the region had not back-switched during the time required for the x-ray measurements.

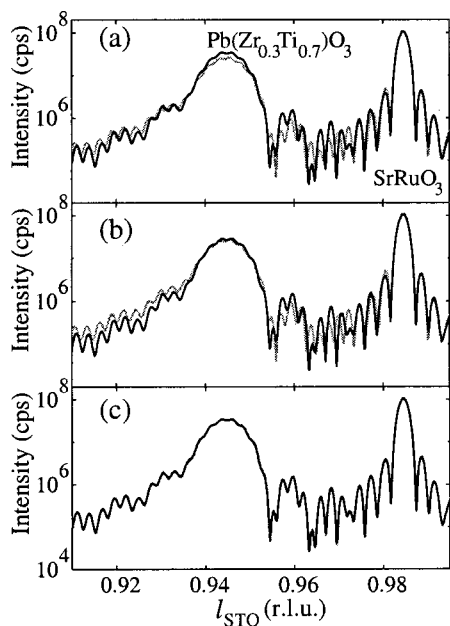


FIG. 3. Comparison of 001 x-ray scattering patterns for a capacitor prepared in the easy and difficult states, before and after fatigue (note the log scale). (a) Comparison between easy (black line) and difficult (gray line) poled states before significant fatigue occurred in the  $I$ - $V$  curves. (b) Comparison of the difficult states before (gray line) and after (black line) fatigue. (c) Comparison of the easy states before and after fatigue. (The profiles are indistinguishable).

The film was poled initially into the difficult state, then the easy state. The x-ray profiles for each state are compared in Fig. 3(a). The significant differences between the scattering profiles in the region of the PZT 001 peak indicated that the microscopic distributions of parallel and antiparallel  $180^\circ$  domains were different, as would be expected for a capacitor poled into opposite states. Also, the PZT 001 peak intensity was significantly less in the difficult state compared to the easy state. This is a characteristic interference effect that indicates that the domain configuration in the state associated with the lower intensity is comprised of a mixture of parallel and antiparallel domains. The higher intensity is associated with a configuration with more unipolar character, i.e., with a smaller fraction of minority domains.<sup>4</sup> If both states were unipolar with opposite polarity, the PZT 001 intensities would be nearly equal, although the profiles near the Bragg peak would differ significantly.

To understand the structural basis of fatigue, the films were switched multiple cycles until the  $I$ - $V$  characteristics showed a significant decrease in the switchable polarization as shown in Fig. 2(b). Imprint was still clearly evident, as was an increase in the leakage current with negative applied voltage. After fatigue, a second pair of x-ray profiles was measured. As shown in Figs. 3(b)-3(c), the scattering pattern for the fatigued difficult state differed from its original unfatigued profile, while those for the two easy states were indistinguishable. In a separate experiment, x-ray CTR profiles were taken on a sample that had similar electrical characteristics and strong imprint, but was not fatigued between the

pairs of x-ray measurements. In agreement with the first sample, the initial scattering profiles for a difficult and easy configuration exhibited significant differences, and the PZT 001 peak intensity comparisons indicated that the difficult state was a mixed domain configuration. However, in contrast to the fatigued sample, the scattering patterns from the unfatigued capacitor poled at separate times into its difficult state were indistinguishable, as were the scattering patterns from each preparation into the easy state.

These scattering results suggest the following picture for the structural nature of fatigue in epitaxial PZT films. The easy state is predominantly unipolar, whereas the difficult state is mixed. During fatigue, the easy state remains unipolar, while the difficult state contains fewer and fewer domains antiparallel to the easy direction. This is consistent with the nucleus inhibition model<sup>1</sup> in which the decrease in switchable polarization occurs through the suppression of the formation of minority domains antiparallel to an unipolar matrix. Our results are inconsistent with others models of fatigue such as bulk pinning, development of a passive layer, or the appearance of  $90^\circ$  domains. We note that the x-ray technique used in this study determines the polarity of the film through a direct structural measurement that is sensitive to the entire domain configuration. This is complementary to the electrical measurements that are sensitive only to those domains that contribute to the switchable polarization, and the AFM measurements, that image the piezoresponse of small areas.

This work is supported by the State of Illinois under HECA, the U.S. Department of Energy, Basic Energy Sciences—Materials Science under Contract No. W-31-109-ENG-38, the David and Lucille Packard Fellowship, and the NSF DMR-9973801.

- <sup>1</sup>E. L. Colla, D. V. Taylor, A. K. Tagantsev, and N. Setter, *Appl. Phys. Lett.* **72**, 2478 (1998).
- <sup>2</sup>E. L. Colla, S. Hong, D. V. Taylor, A. K. Tagantsev, N. Setter, and K. No, *Appl. Phys. Lett.* **72**, 2763 (1998).
- <sup>3</sup>B. G. Chae, C. H. Park, Y. S. Yang, and M. S. Jang, *Appl. Phys. Lett.* **75**, 2135 (1999).
- <sup>4</sup>C. Thompson, C. M. Foster, J. A. Eastman, and G. B. Stephenson, *Appl. Phys. Lett.* **71**, 3516 (1997).
- <sup>5</sup>C. M. Foster, G. R. Bai, R. Csencsits, J. Vetrone, R. Jammy, L. A. Wills, E. Carr, and J. Amano, *J. Appl. Phys.* **81**, 2349 (1997).
- <sup>6</sup>C. B. Eom, R. J. Cava, R. M. Fleming, J. M. Phillips, R. B. vanDover, J. H. Marshall, J. W. P. Hsu, J. J. Krajewski, and J. W. F. Peck, *Science* **258**, 1766 (1992).
- <sup>7</sup>C. M. Foster, Z. Li, M. Buckett, D. Miller, P. M. Baldo, L. E. Rehn, G. R. Bai, D. Guo, H. You, and K. L. Merkle, *J. Appl. Phys.* **78**, 2607 (1995).
- <sup>8</sup>J. S. Speck, A. C. Daykin, A. Seifert, A. E. Romanov, and W. Pompe, *J. Appl. Phys.* **78**, 1696 (1995).
- <sup>9</sup>R. Feidenhans'l, *Surf. Sci. Rep.* **10**, 105 (1989).
- <sup>10</sup>F. Bauer, *Ferroelectrics* **49**, 213 (1983).
- <sup>11</sup>G. Pike, W. L. Warren, D. Dimos, B. A. Tuttle, R. Ramesh, J. Lee, V. G. Keramidas, and J. T. Evans, Jr., *Appl. Phys. Lett.* **66**, 484 (1995).
- <sup>12</sup>J. Lee and R. Ramesh, *Appl. Phys. Lett.* **68**, 484 (1996).
- <sup>13</sup>K. Ghosh, S. Streiffner, O. Auciello, G. R. Bai, Q. Gan, C. B. Eom, and C. Thompson, *Mat. Res. Soc. Fall Mtg. Abstracts*, 1999, p. 438.
- <sup>14</sup>R. Bruchhaus, D. Pitzer, R. Priming, W. R. Wersing, and Y. Xu, *Integr. Ferroelectr.* **14**, 141 (1997).